

Spatial dependence of ultrafast carrier recombination centers of phosphorus-implanted and annealed silicon wafers

Andreas Othonos^{a)} and Constantinos Christofides

Department of Physics, University of Cyprus, P.O. Box 20537, 1678 Nicosia, Cyprus

(Received 19 December 2001; accepted for publication 5 June 2002)

In this letter, the spatial dependence of the carrier recombination centers induced in phosphorus-implanted and annealed silicon wafers have been examined. Ultrafast time-resolved reflectivity measurements of a set of phosphorus-implanted annealed silicon wafers ($10^{16} \text{ P}^+/\text{cm}^2$) as a function of position on the wafer have been carried out, and an x - y map of the carrier lifetime for each of the samples has been obtained. Measurements reveal distinct features of the distribution of carrier recombination centers for the nonannealed and annealed samples between 350°C and 1100°C in an area of $36 \times 36 \mu\text{m}^2$ with resolution better than $3 \mu\text{m}$. The presence of islands of clusters in ion-implanted and annealed samples is also discussed in this letter. © 2002 American Institute of Physics. [DOI: 10.1063/1.1497723]

The recent demand for high-speed microelectronic and optoelectronic devices with an ultrafast response has given a renewed interest in the area of implantation.¹⁻³ Although crystalline silicon has a slow response, it is known that amorphous silicon^{4,5} and amorphization due to an ion implantation process⁶ alter the temporal behavior in these materials. Amorphous silicon has been reported with an ultrafast response shorter than picosecond due to its short free-carrier lifetime. The reduction of the free-carrier lifetime is the result of the introduction of defects into the crystalline semiconductor, which act as traps and recombination centers. The objective of this work is the study of the annealing effect of highly implanted silicon through measurements of spatial dependence of the ultrafast relaxation of photogenerated carriers. Comparisons with other studies made on the same materials will also be performed.^{2,7-9}

As it is well known, above band gap, direct or indirect optical excitation of semiconductors generates electrons and holes. The dynamics of these photogenerated carriers can be monitored directly using time-resolved reflectivity measurements.¹⁰ The present work reports on the spatial dependence of the recombination centers and their behavior as a function of annealing temperature.

The experimental setup utilized a collinear pump-probe reflectivity arrangement commonly used in ultrafast time-resolved Raman scattering.^{11,12} A mode-locked, Ti:Sapphire laser (Spectra-Physics, Tsunami), pumped by a solid-state laser (Millennia) produced 80 fs pulses and was tuned at 790 nm. The experimental arrangement was used to separate the incident laser beam into two perpendicular polarized beams: the pump, and the probe. The optical elements in the experimental arrangement were carefully selected to have minimum dispersion effect on the optical pulse duration thus maintaining maximum temporal resolution. A beam splitter pellicle was used to recombine the pump and probe into a collinear beam that was focused with an objective lens to a spot $< 1.5 \mu\text{m}$ radius onto the sample. The reflected pump-

probe beams from the sample were then directed from the pellicle beam splitter onto a polarizer cube, which separated the reflection of the probe and the pump beams. The reflection from the probe beam was directed onto a silicon photodiode, which was processed with a lock-in amplifier. Under the excitation condition of the experiment, no apparent damage was induced on the samples.

The samples used in these experiments are silicon wafers lightly doped with boron ($20\text{--}25 \Omega\text{cm}$) implanted at 150 keV with phosphorus at doses of $1 \times 10^{16} \text{ P}^+/\text{cm}^2$ through a thin oxide layer at room temperature. After implantation, the thin oxide layer was removed and wafers were cut along the crystallographic axes into several samples. These samples were then thermally annealed isochronically at various temperatures starting between 350°C and 1100°C for 1 h in nitrogen atmosphere. The damage induced depth of the samples was estimated from modeling of the implantation to be approximately $0.3 \mu\text{m}$.¹³ The samples were positioned on computer controlled motorized x - y translation stage with $0.1 \mu\text{m}$ resolution. This allowed time-resolved measurements to be taken along each of the samples at $3 \mu\text{m}$ steps covering an area of $36 \times 36 \mu\text{m}$. Measurements with smaller step intervals were also attempted. However, due to the $3 \mu\text{m}$ diameter spot size resolution, no information was gained.

The data exhibit a fast rise followed by a recovery back toward equilibrium reflectivity. The relatively fast recovery of the reflectivity is attributed to the recombination centers generated from the defects due to the ion implantation. Monitoring the carrier lifetime in these samples will be in effect a measure of the recombination centers present at the area of the probing beam. The absolute value of the maximum change in reflectivity that varies with the annealing temperature of the implanted samples is approximately 10^{-4} . We should point out that this change in reflectivity increased linearly with pump power intensity up to several times the working intensity of the experiment, with nonlinear phenomena noticeable.

The variation of the carrier lifetime as a function of the annealed temperatures on these samples and the carrier kinetics in these systems has been discussed elsewhere.¹⁰ The

^{a)}Electronic mail: othonos@ucy.ac.cy

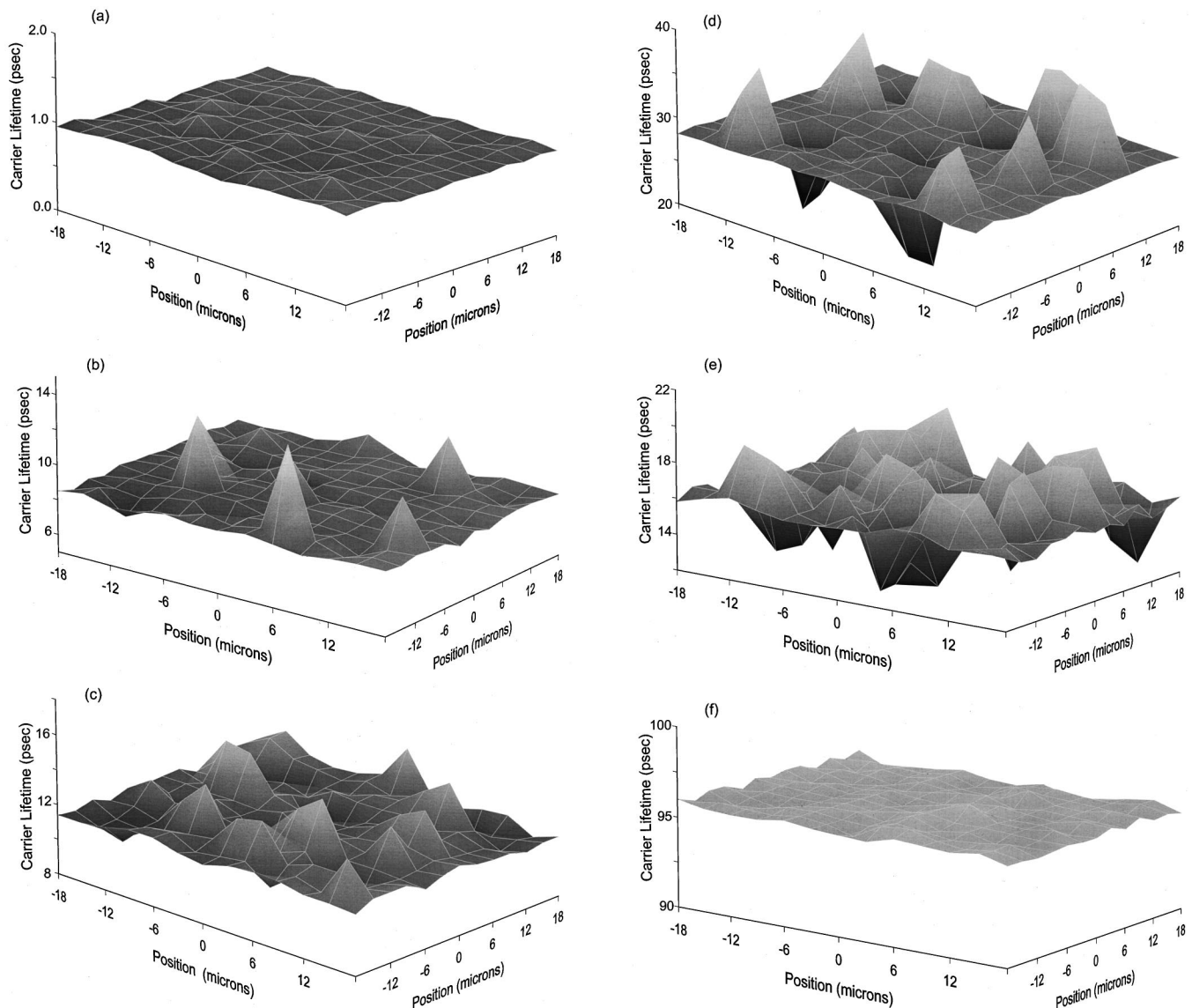


FIG. 1. Carrier lifetime of the silicon implanted annealed at (a) nonannealed, (b) 350 °C, (c) 500 °C, (d) 700 °C, (e) 900 °C, and (f) 1100 °C, sample as function of the position on the sample. The graph maps out an area of $36 \times 36 \mu\text{m}$ with spatial step of $3 \mu\text{m}$ and spot size radius of $1.5 \mu\text{m}$. The experimental error on carrier lifetime (z axis) is approximately $\pm 6\%$.

subject of this work is the spatial distribution of the carrier lifetime, or, in effect, the morphology of the carrier recombination centers with annealing temperature on the ion-implanted wafer samples. The carrier lifetime was obtained through fitting exponential decays onto the experimental data. Carrier lifetime was measured over the entire scanned area for the nonannealed and various annealed samples. These data are shown in Fig. 1. The error in the carrier lifetime data was estimated to be approximately $\pm 6\%$.

Figure 1(a) shows spatial profile of the carrier lifetimes obtained over an area of $36 \times 36 \mu\text{m}$ close to the center of the nonannealed phosphorus implanted silicon sample. Here, we should point out that similar morphological pictures have been observed in all parts of the wafer. The variation over the sample area of the carrier lifetime that in effect is the variation of the recombination centers due to the defects induced from the ion implantation is very small. Specifically, the average value of the carrier lifetime is approximately 0.97 ps with standard deviation of 0.04 and a minimum and maximum of 0.86 and 1.09 ps, respectively. The carrier lifetime

seems to be homogeneous around the whole implanted wafers. In fact the high implanted and nonannealed samples appear to have a flat distribution of implanted defects. Variations due to defect clusters in these samples are undetectable under the present resolution since they have diameter less than 1 nm according to Nelson.¹⁴

In the next few figures the annealed implanted data will be shown. In contrast to the data seen in Fig. 1(a) for the nonannealed sample, the three-dimensional graphs for the annealed samples appear to have some interesting structure. Figure 1(b) shows the carrier lifetime over a similar area for the ion-implanted sample annealed at 350 °C. Although the morphological distribution of the carrier lifetime appears to be flat (~ 8.6 ps), there are some distinct hills and valleys. The hills correspond to defects that have a lower annihilation threshold giving larger carrier lifetime, whereas the valleys correspond to defects with higher annihilation threshold resulting in shorter carrier lifetime (closer to the values of the nonannealed sample). What is interesting in these results is the fact that these hills and valleys appear to be of the order

of $\sim 2 \mu\text{m}$ diameter corresponding to a group or cluster of defects or recombination centers. Although these hills or valleys appear to be few, they may cause problems, where this material may be used for its ultrafast response where a few micron spatial resolution is required. On the other hand, if the spot size of the incident beam is large enough ($>30 \mu\text{m}$), then the aforementioned changes average out over the response of all the material. The size of such clusters (at 150 keV and dose of $1 \times 10^{16} \text{ cm}^{-2}$) is of the order of 140 Å and this was found and published almost twenty years ago.¹⁴ Here, it appears that an island of clusters can have a size of 2 μm . Such islands can be formed because of a certain potential difference developed by the presence of dislocations and impurities. For these measurements, the average value for the carrier lifetime is 8.6 ps with a standard deviation of 0.7 ps, minimum of 6.4 ps and maximum of 13.7 ps.

With increasing annealing temperature, the carrier lifetime increased (~ 18 ps) as the defects were removed.¹⁰ In Fig. 1(c), one can note that a further increase of the annealing temperature to 500 °C resulted in a decrease in the carrier lifetime due to the well-known effect of reverse annealing. The average lifetime was approximately 11.6 ps. What we notice here is that the carrier lifetime distribution over the scanned area, and, thus, the recombination centers distribution, is much rougher than the distribution observed on a sample annealed at 350 °C. This behavior is due to the clustering of defects, which is responsible for the negative annealing. The clustering of defects formed around the 500 °C annealing temperature brings the carrier lifetime to a value, lower than expected, whereas the observed hills are more likely areas of nonclustering formation. On the other hand, the diameter of the cluster regions is larger than in the case of lower annealed sample. This phenomenon has also been described by Nelson¹⁵ where it has been shown that the dimension of the cluster increases as a function of temperature. For these measurements, the average carrier lifetime is approximately 11.6 ps with a standard deviation of 0.9 ps, minimum 9.4 ps, and maximum 14.5 ps.

At higher annealing temperature, we have further annihilation of the recombination centers resulting to longer carrier lifetimes [Fig. 1(d)]. The morphology of the scanned area shows relatively constant distribution of recombination centers. However, there are several large hills and valleys. The hills correspond to defects with a lower annihilation threshold and the valleys with defects with higher annihilation threshold. An interesting note here is the size of the hills and valleys that are larger, both in depth and area, than the hills and valleys observed at lower annealing temperatures. In fact, at high-temperature annealing, the defect phenomena in implanted semiconductors are not governed by clusters but by line and loops dislocations. The mixture of hills and valleys in Fig. 1(f) are results of the dislocation defects. A further increase in annealing temperature, of the ion-implanted silicon samples to 900 °C results in a noticeable reduction of the carrier lifetime [Fig. 1(e)]. This relatively fast relaxation of the carriers is attributed to the formation of dislocation loops, which act as recombination centers. The

morphological structures of these dislocation loops appear to be rougher than the recombination centers observed at lower temperatures. These results are in a good agreement with various electrical, photothermal, and optical measurements performed on the same samples in the past.^{3,7-9,13}

Finally, at the highest-annealing temperature, namely at 1100 °C, the samples behave like normal crystalline silicon with the lifetime of the photoexcited carriers being 95 ps. This value is close to the measured carrier lifetime of the nonimplanted silicon. The morphology of the carrier lifetime in this high-temperature annealed sample is flat as shown in Fig. 1(f). This suggests that, as expected, there are very little fluctuations in the carrier lifetime over the scanned area on the sample, since most of the recombination centers have been removed. Nevertheless, it is important to note that we observe a drastic change in the carrier lifetime between 900 °C and 1100 °C, a fact that shows the high sensitivity of the ultrafast technique relative to other conventional characterization techniques.^{16,17}

In summary, we have investigated the spatial dependence of the carrier recombination centers with micron resolution in highly implanted annealed silicon samples through the measurements of ultrafast time resolved reflectivity. The main results of this study can be summarized as follows: (a) strong influence of thermal annealing to the $x-y$ map of the carrier recombination centers and (b) rougher $x-y$ spatial distribution of the carrier recombination centers with increasing annealing temperature.

This work has been supported by the Research Promotion Foundation of the Government of Cyprus under the "IENEK 14/2000."

¹H. Ryssel and I. Ruge, *Ion Implantation* (Wiley, Toronto, 1986).

²C. Christofides and G. Ghibaudo, *Effects of Disorder and Defects in Ion-Implanted Semiconductors: Optical and Photothermal Characterization*, Semiconductors and Semimetals Vol. 46 (Academic, New York, 1997).

³G. Ghibaudo and C. Christofides, *Effects of Disorder and Defects in Ion-Implanted Semiconductors: Electrical and Physicochemical Characterization*, Semiconductors and Semimetals Vol. 45 (Academic, New York, 1997).

⁴J. Kubhl, E. O. Gobel, T. Pfeiffer, and A. Jonietz, *Appl. Phys. A: Solids Surf.* **34**, 105 (1984).

⁵O. B. Wright, U. Zammit, M. Marinelli, and V. E. Gusev, *Appl. Phys. Lett.* **69**, 553, (1996).

⁶F. E. Doany, D. Grischkowsky, and C. C. Chi, *Appl. Phys. Lett.* **50**, 460, (1987).

⁷M. Nestoros, B. C. Forget, C. Christofides, and A. Seas, *Phys. Rev. B* **51**, 14115 (1995).

⁸A. Seas and C. Christofides, *Appl. Phys. Lett.* **66**, 3346 (1995).

⁹A. Othonos and C. Christofides, *J. Appl. Phys.* **78**, 796 (1995).

¹⁰A. Othonos and C. Christofides, *Ultrafast dynamics in phosphorus implanted silicon wafers: the effects of annealing*

¹¹A. Othonos, *Appl. Phys. Rev.* **83**, 1789 (1998).

¹²A. Othonos, H. M. van Driel, J. F. Young, and P. J. Kelly, *Phys. Rev. B* **43**, 6682 (1991)

¹³A. Othonos, C. Christofides, J. Boussey-Said, and M. Bisson, *J. Appl. Phys.* **75**, 8032 (1994).

¹⁴S. Prussin, D. Margolese, and R. Tauber, *J. Appl. Phys.* **57**, 180 (1985).

¹⁵R. S. Nelson, *Proceedings of the European Conference on ion implantation Stevenage, Herts, England, 1970*, p. 212.

¹⁶C. Christofides, *Semicond. Sci. Technol.* **7**, 1283 (1992).

¹⁷C. Christofides, H. Jaouen, and G. Ghibaudo, *J. Appl. Phys.* **65**, 4832 (1989).